Porter, J. G., Fuller, F., Cordell, B., Arfsten, A., Lewicki, J. A., & Schenk, D. B. (1987) *Fed. Proc., Fed. Am. Soc. Exp. Biol. 46*, 1132.

Scarborough, R. M., Schenk, D. B., McEnroe, G. A., Arfsten, A., Kang, L.-L., Schwartz, K., & Lewicki, J. A. (1986) *J. Biol. Chem. 261*, 12960-12964.

Schenk, D. B., Johnson, L. K., Schwartz, K., Sista, H., Scarborough, R. M., & Lewicki, J. A. (1985a) *Biochem. Biophys. Res. Commun. 127*, 433-442.

Schenk, D. B., Phelps, M. N., Porter, J. G., Scarborough, R. M., McEnroe, G. A., & Lewicki, J. A. (1985b) *J. Biol. Chem. 260*, 14887-14890.

Schenk, D. B., Phelps, M. N., Porter, J. G., Fuller, F., Cordell, B., & Lewicki, J. A. (1987) *Proc. Natl. Acad. Sci. U.S.A. 84*, 1521-1525.

Shimonaka, M., Saheki, T., Hagiwara, H., Ishido, M., Nogi, A., Fujita, T., Wakita, K.-I., Inada, Y., Kondo, J., & Hirose, S. (1987) *J. Biol. Chem. 262*, 5510-5514.

Smith, P. K., Krohn, R. I., Hermanson, G. T., Mallia, A. K., Gartner, F. H., Provenzano, M. D., Fujimoto, E. K., Goeke, N. M., Olson, B. J., & Klenk, D. C. (1985) *Anal. Biochem. 150*, 76-85.

Steiner, A. L., Parker, C. W., & Kipnis, D. M. (1972) *J. Biol. Chem. 247*, 1106-1113.

Takayanagi, R., Inagami, T., Snajdar, R. M., Imada, T., Tamura, M., & Misono, K. S. (1987) *J. Biol. Chem. 262*, 12104-12113.

Vandlen, R. L., Arcuri, K. E., & Napier, M. A. (1985) *J. Biol. Chem. 260*, 10889-10892.

White, A. A., & Zenser, T. V. (1971) *Anal. Biochem. 41*, 372-396.

Yip, C. C., Laing, L. P., & Flynn, T. G. (1985) *J. Biol. Chem. 260*, 8229-8232.

Fourier Transform Infrared Study of Fully Hydrated Dimyristoylphosphatidylglycerol. Effects of Na^+ on the *sn*-1′ and *sn*-3′ Headgroup Stereoisomers

Timo I. Lotta, Ilkka S. Salonen, Jorma A. Virtanen, Kari K. Eklund, and Paavo K. J. Kinnunen*

Department of Membrane Physics, KSV Research Laboratories, Helsinki, Finland

Received February 25, 1988; Revised Manuscript Received June 2, 1988

ABSTRACT: Molecular packing and the thermotropic phase behavior of fully hydrated ammonium salts of 1,2-dimyristoyl-*sn*-glycero-3-phosphatidyl-*sn*-1′-glycerol (1′-DMPG) and the corresponding 3′ stereoisomer (3′-DMPG) as well as the effects of 300 mM NaCl on these lipids were studied by Fourier transform infrared (FTIR) spectroscopy. The ammonium salts of both stereoisomers show similar thermotropic phase behavior and have an order–disorder phase transition at approximately 21 °C. While complexing with Na^+, however, an incubation of liposomes at +6 °C for 3 days results in significant structural differences between liposomes of 1′-DMPG and 3′-DMPG. In the presence of 300 mM NaCl the infrared spectra for 3′-DMPG reveal the appearance of a more solidified lipid nominated here as the highly crystalline phase with a transition into the liquid-crystalline state at a significantly higher temperature (approximately at 33 °C) than that for 1′-DMPG (approximately at 23 °C). Crystal field splitting resulting from interchain vibrational coupling is observed in the CH_2 scissoring mode of the 3′-DMPG(Na^+) complex in the highly crystalline phase ($T < 33$ °C); i.e., the acyl chains are packed in a rigid orthorhombic- or monoclinic-like crystal lattice. At temperatures above the transition at 33 °C the acyl chains of 3′-DMPG(Na^+) give rise to infrared spectra indicative of hexagonal packing. The latter type of hydrocarbon chain packing is also found for the ammonium salts of 1′-DMPG and 3′-DMPG without Na^+ as well as for 1′-DMPG with Na^+. In addition, the binding of Na^+ to 3′-DMPG causes narrowing of the bands associated with the interfacial and polar headgroup regions of 3′-DMPG and thus reveals reduced motional freedom. This demonstrates that Na^+ binds tightly to 3′-DMPG, leading to the immobilization of the entire phospholipid polar headgroup. Such effects by Na^+ are not observed for 1′-DMPG.

Interactions of metal cations with membrane phospholipids have recently been the focus of increasing interest. This is due to observations that in membranes containing negatively charged phospholipids changes in membrane morphology (Verkleij et al., 1984), fluidity (Träuble et al., 1976), and phospholipid phase transitions (Watts et al., 1978; Jähnig, 1976; Träuble, 1977) can be triggered isothermally by changing the ionic strength, pH, or membrane potential (Kinnunen & Virtanen, 1986). Thus, the lipid–ion interactions are likely to play an important role in the regulation of the structure and function of biological membranes.

Characteristically lipid–cation interactions induce tighter packing of the acyl chains and stabilization of the bilayer, resulting in increased phase transition temperature and enthalpy (Amey & Chapman, 1983). Ca^{2+} in particular has long been recognized as a fusion-promoting agent. Its mode of interaction is based on its complexing to the headgroup moieties of membrane lipids. FTIR[1] spectroscopy has been

---

* Address correspondence to this author at Department of Membrane Physics, KSV Research Laboratories, KSV Chemical Corp., POB 128, SF-00381 Helsinki, Finland.

0006-2960/88/0427-8158$01.50/0 © 1988 American Chemical Society

used to study the effects of Ca^{2+} on the structure of phosphatidylserine (PS) vesicles (Dluhy et al., 1983). Casal et al. (1987a,b) have characterized the thermotropic phase behavior of PS complexed with Li^+ and Ca^{2+}. As judged by the infrared data Li^+ and Ca^{2+} form crystalline complexes with PS and introduce a more ordered lipid phase with a gel to liquid-crystalline phase transition at much higher temperatures than those of other salts of PS. The dried (anhydrous) samples of PS–Li^+ and PS–Ca^{2+} complexes were recently characterized (Casal et al., 1987c). The complexation of DMPS with mono- and divalent cations has also been studied by differential scanning calorimetry (DSC) and X-ray diffraction (Hauser et al., 1982; Hauser & Shipley, 1981, 1983, 1984).

Studies on cation-induced processes have increasingly focused on phosphatidylglycerol (PG), which is a negatively charged phospholipid abundant in plants and bacterial membranes and in mammalian lung surfactant (Boggs & Rangaraj, 1983; Tocanne et al., 1974; Cevc et al., 1980; Eklund & Kinnunen, 1986; Eisenberg et al., 1979; Laghdar-Ghazal et al., 1983; Sacre & Tocanne, 1977; Smirnova et al., 1986; Borle & Seelig, 1985; Wilkinson et al., 1987). The interaction of PG with metal ions has been demonstrated experimentally mainly by DSC and monolayer techniques (Borle & Seelig, 1985, and references cited therein). Farren and Cullis (1980) characterized the behavior of DMPG–Ca^{2+} using ^{31}P NMR spectroscopy. The most conspicuous effect of Ca^{2+} was an increase in the temperature of the gel to liquid-crystalline phase transition (Borle & Seelig, 1985). The conformation and molecular packing properties of sodium rac′-DMPG have been determined by X-ray analysis of single crystals (Pascher et al., 1987). In these studies the synthetic phosphatidylglycerols used have generally been racemic with respect to the polar headgroup glycerol (Joutti & Renkonen, 1976). The only naturally occurring polar headgroup stereoisomer of PG is the *sn*-3-phosphatidyl-*sn*-1′-glycerol.

Less attention has been given to the role of the polar headgroup stereoconfiguration in the phase behavior of PG, and only a few studies have employed stereochemically well-defined lipids (Eklund et al., 1987; Wohlgemüth et al., 1980). Recently in our laboratory significant differences were evident in the Na^+-induced aggregation of 1′-DMPG and 3′-DMPG. Our DSC data show that the thermotropic phase behavior of 1′-DMPG and its 3′ stereoisomer differ after the samples are incubated with NaCl at temperatures below the pretransition temperature of DMPG.[2] In the presence of NaCl 3′-DMPG forms a highly crystalline phase that has a melting enthalpy about 3–4 times that of 3′-DMPG(NH_4^+) and a transition temperature about 10 °C higher than the gel to liquid-crystalline phase transition of 3′-DMPG(NH_4^+) incubated without Na^+.[2] Similar metastable phase behavior has been shown for PE. Upon prolonged incubation of PE a crystalline phase is formed that behaves like the highly crystalline phase observed for 3′-DMPG(Na^+) (Wilkinson & Nagle, 1984; Chang & Epand, 1983; Seddon et al., 1983). The crystalline phase of PE is also formed without incubation in cold if the liposomes are hydrated below T_m (Mantsch et al., 1983).

The results of the FTIR spectroscopic measurements on the thermotropic phase behavior of 1′-DMPG(NH_4^+) and 3′-DMPG(NH_4^+) in buffer containing zero or 300 mM NaCl reported here supplement our liposomal aggregation and DSC data regarding the structure and dynamics of the Na^+–PG interactions, i.e., the effect of PG polar headgroup stereoisomers in the membrane properties of this lipid.

MATERIALS AND METHODS

The ammonium salts of 1,2-dimyristoyl-*sn*-glycero-3-phosphatidyl-*sn*-1′-glycerol (1′-DMPG) and the corresponding 3′ stereoisomer (3′-DMPG) were from KSV Chemical Corp. (Helsinki, Finland). The ammonium salt of 1,2-dimyristoyl-*sn*-glycero-3-phosphatidyl-*rac*′-glycerol (rac′-DMPG) was a product of Sigma. No impurities were detected in these lipids upon thin-layer chromatography on silica gel (Merck AG, Darmstadt, West Germany) using the solvent mixture $CHCl_3/CH_3OH/H_2O/NH_3$ (65:20:2:2 v/v). The water used was freshly deionized in a Milli-RO/Milli-Q (Millipore, Bedford, MA) filtering system.

Liposomes were prepared as follows. Stock solutions of the lipids were made in chloroform. The solvent was removed under a stream of nitrogen, whereafter the sample was maintained under reduced pressure overnight. The dry lipid was hydrated to yield a final concentration of 8 mg/mL in 50 mM Tris-HCl and 0.5 mM EDTA, pH 7.4, buffer. When indicated, 300 mM NaCl was included. The hydrated lipids were suspended by vortexing repeatedly (0.5–1 min) and sonicating (1–2 min) on a Bransonic 221 bath-type irradiator at 45 °C. The samples were then incubated at +6 °C for 3 days before the infrared measurements.

Infrared spectra were collected at 4-cm^{-1} resolution with a Nicolet 60SX spectrophotometer equipped with a room temperature deuteriated triglycine sulfate (DTGS) detector with KBr windows. For each spectrum, 2000 scans were co-added and apodized with the Happ–Genzel function. For liquid samples the Circle Cell (a cylindrical attenuated total reflectance cell) with a ZnSe crystal at 45° angle of incidence was employed (Spectra-Tech, Stanford, CT). Due to sedimentation of the liposomes during the experiments, comparison of intensities of the vibrational bands could not be carried out. To assure matching of both the path length and temperature during the subtraction of water bands the spectrum of the buffer was also recorded at 0.5 °C intervals over the range 6–50 °C by using the same experimental conditions as outlined above for the lipid samples. The sample cell was mounted in a jacket constructed in our laboratory and thermostated with a Lauda RC6 water circulator. Temperature was monitored with a Lauda Pt 100 sensor inserted into the jacket. The overall accuracy of temperature control was within ±0.1 °C. For temperature scanning we constructed a computer-controlled heating/cooling system. The computer of the FTIR spectrophotometer was interfaced to the Lauda RC6 circulator; i.e., the computer automatically controls the temperature and recording of the spectra.

The peak positions were determined by the peak-picking routine supplied with the FTIR software by Nicolet. We have also written our own programs for the determination of peak

---

[1] Abbreviations: 1′-DMPG, 1,2-dimyristoyl-*sn*-glycero-3-phosphatidyl-*sn*-1′-glycerol; 3′-DMPG, 1,2-dimyristoyl-*sn*-glycero-3-phosphatidyl-*sn*-3′-glycerol; rac′-DMPG, 1,2-dimyristoyl-*sn*-glycero-3-phosphatidyl-*rac*′-glycerol; DPPC, 1,2-dipalmitoyl-*sn*-glycero-3-phosphatidylcholine; PPDPC, 1-palmitoyl-2-[10-(pyren-1-yl)decanoyl]-*sn*-glycero-3-phosphatidylcholine; PG, phosphatidylglycerol; PE, phosphatidylethanolamine; PS, phosphatidylserine; DSC, differential scanning calorimetry; FTIR, Fourier transform infrared spectroscopy; DTGS, deuteriated triglycine sulfate; T_m, main transition temperature; T_{pre}, pretransition temperature; T_{hc}, highly crystalline transition temperature (from highly crystalline to liquid crystalline); EDTA, ethylenediaminetetraacetic acid; Tris, tris(hydroxymethyl)aminomethane; 1′-DMPG(NH_4^+), 1′-DMPG hydrated as an ammonium salt; 1′-DMPG(Na^+), 1′-DMPG hydrated as an ammonium salt with 300 mM NaCl; 3′-DMPG(NH_4^+), 3′-DMPG hydrated as an ammonium salt; 3′-DMPG(Na^+), 3′-DMPG hydrated as an ammonium salt with 300 mM NaCl.

[2] I. S. Salonen, K. K. Eklund, J. A. Virtanen, and P. K. J. Kinnunen, submitted for publication.

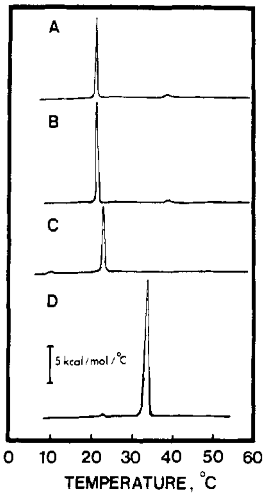

FIGURE 1: DSC traces of liposomes of 1′-DMPG and 3′-DMPG. The samples were incubated at +6 °C for 3 days: (A) 1′-DMPG(NH_4^+); (B) 3′-DMPG(NH_4^+); (C) 1′-DMPG(Na^+); (D) 3′-DMPG(Na^+). A high-sensitivity DSC MC-2 (Microcal Inc., Northampton, MA) was used at a scanning rate of 0.5 °C/min. Lipid concentration was 1 mg/mL (cf. Materials and Methods).

positions. Base-line leveling was performed when necessary. Smoothing procedures were not used. The IRDCON program by Nicolet was used to enhance spectral resolution (Fourier self-deconvolution).

RESULTS AND DISCUSSION

In Figure 1 are shown DSC traces of 1′- and 3′-DMPG liposomes prepared as ammonium salts as well as in the presence of 300 mM NaCl. The samples were incubated at +6 °C for 3 days. In the absence of NaCl the thermotropic behavior of 1′- and 3′-DMPG is similar with a main transition at 21.1 °C and ΔH of 6.5 kcal/mol. The minor peak that appears at approximately 38.5 °C is nominated as the post-transition.[2] Figure 1C displays a DSC trace for 1′-DMPG in the presence of 300 mM NaCl. The characteristic peak of the order–disorder phase transition is seen at 22.9 °C with an enthalpy of 5.8 kcal/mol. The pretransition for 1′-DMPG(Na^+) is observed at approximately 11 °C. Our infrared data do not reveal any changes at T_{pre}. However, the DSC trace of 3′-DMPG(Na^+) differs significantly from that of 1′-DMPG(Na^+). There is a peak at 33.6 °C (T_{hc}) with an enthalpy of approximately 19 kcal/mol (Figure 1D). This peak corresponds to the melting of the more ordered highly crystalline phase. More detailed description of the polymorphic phase behavior of 1′- and 3′-DMPG and their mixtures as revealed by DSC will be given elsewhere.[2]

Although calorimetric data provide good evidence for the different types of thermotropic phase transitions, spectroscopic studies can indicate which parts of the phospholipid molecules are involved. The infrared spectra of phospholipids can be conveniently separated into spectral regions that originate from the polar headgroup, the interfacial region, or the nonpolar hydrocarbon tails. In the following we examine in detail the CH_2 stretching and scissoring modes, the C=O stretching mode, and the vibrations due to the polar headgroup region for 1′- and 3′-DMPG by analyzing the infrared spectra recorded both in the absence and in the presence of 300 mM NaCl. In Table I are summarized the temperatures (determined by DSC and IR) of the phase transitions for 1′- and 3′-DMPG as ammonium salts hydrated in buffer containing zero or 300 mM NaCl.

Table I: Temperatures of the Phase Transitions (T_m and T_{hc}) Observed for 1′-DMPG(NH_4^+) and 3′-DMPG(NH_4^+) Liposomes[a]

	gel to liquid crystalline			highly crystalline to liquid crystalline		
	IR	DSC		IR	DSC	
	T_m (°C)	T_m (°C)	ΔH (kcal/mol)	T_c (°C)	T_c (°C)	ΔH (kcal/mol)
1′-DMPG-(NH_4^+)	20.6	21.1	6.5			
1′-DMPG-(Na^+)	22.8	22.9	5.8			
3′-DMPG-(NH_4^+)	20.7	21.1	6.5			
3′-DMPG-(Na^+)				32.9	33.6	19

[a] The samples were incubated for 3 days at +6 °C. The transition temperatures were determined by DSC and infrared spectroscopy (employing the symmetric CH_2 stretching mode).

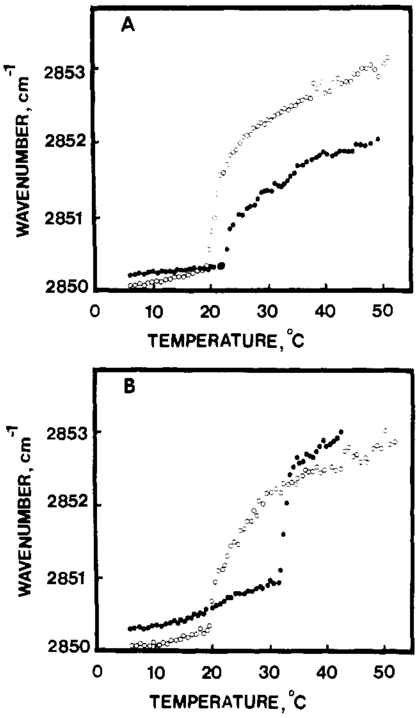

FIGURE 2: Temperature dependence of the wavenumber of the symmetric CH_2 stretching band: (A) 1′-DMPG(NH_4^+) (○) and 1′-DMPG(Na^+) (●); (B) 3′-DMPG(NH_4^+) (○) and 3′-DMPG(Na^+) (●).

Comparison of the Infrared Spectra of 1′-DMPG(NH_4^+) and 3′-DMPG(NH_4^+). (*a*) *Acyl Chain Bands.* Two strong vibrational bands dominate the 3000–2800-cm^{-1} spectral region of both 1′- and 3′-DMPG liposomes, assigned to the asymmetric methylene stretching mode at approximately 2920 cm^{-1} and the symmetric methylene stretching mode near 2850 cm^{-1}. The asymmetric and symmetric stretching modes of the terminal methyl groups are observed at approximately 2950 and 2870 cm^{-1}, respectively (Casal & Mantsch, 1984). Unfortunately, the latter two modes are weak in intensity in both 1′- and 3′-DMPG liposomes and thus inaccessible to closer characterization. The thermotropic behavior of the wavenumber of the symmetric CH_2 stretching mode is displayed for 1′-DMPG(NH_4^+) and 3′-DMPG(NH_4^+) in Figure 2; the temperature profiles are similar for both isomers. The advantage of monitoring the symmetric CH_2 rather than the asymmetric CH_2 stretching is that although the overall change in wavenumber and bandwidth is even larger for the latter mode, the former is less overlapped with other vibrational modes (Casal & Mantsch, 1984).

Table II: Infrared Absorption Bands (cm^{-1}) in the CH Stretching, CH_2 Scissoring, C=O Stretching, and the Polar Headgroup Region of Ammonium Salts of 1′-DMPG, 3′-DMPG, and rac-DMPG in Solid Phase

	solid[b]		
assignment[a]	1′-DMPG	3′-DMPG	rac′-DMPG
OH stretch (hydrogen bonded)	3218	3215	3216
asym CH_3 stretch	2956	2956	2956
asym CH_2 stretch	2917.9	2917.6	2918.5
sym CH_3 stretch	2873	2873	2873
sym CH_2 stretch	2849.9	2849.9	2850.1
C=O stretch	1739.5	1739.5	1740.1
CH_2 scissoring	1468.0	1468.0	1468.1
asym PO_2^- stretch	1204.5	1205.0	1205.6
asym C—O ester stretch	1170 (sh)	1066 (sh)	1068 (sh)
sym PO_2^- stretch	1109 (sh) 1089.5	1109 (sh) 1091.6	1112 (sh) 1090.3
sym C—O ester stretch	1059.4	1059.0	1058.3
C—OP stretch (phosphate ester stretch)	1048 (sh)	1048 (sh)	1048 (sh)

[a] See Amey and Chapman (1983), Casal and Mantsch (1984), and Casal et al. (1987c). [b] sh = shoulder.

The wavenumber of the symmetric methylene stretching mode of 1′-DMPG(NH_4^+) shows a drastic change from 2850.1 to 2852.7 cm^{-1} at 21 °C and accompanies the main phase transition from gel to liquid-crystalline phase. A sharp shift to higher wavenumbers of the symmetric CH_2 stretching mode was also observed for the 3′-DMPG ammonium salt at 21 °C, indicating the main transition. The half-bandwidth of the symmetric stretching mode of both DMPG headgroup isomers increases as a function of temperature. In the case of 1′-DMPG(NH_4^+) at 10 °C the observed half-bandwidth was approximately 9 cm^{-1}, and at 40 °C it was approximately 13 cm^{-1}. For 3′-DMPG(NH_4^+) the increase in the half-bandwidth of the symmetric stretching mode was approximately 3 cm^{-1}, and the widths at 10 and 40 °C were 8 and 11 cm^{-1}, respectively.

Earlier studies (Casal & Mantsch, 1984) have assigned the half-bandwidth increase to the augmentation of the rotational mobility of the acyl chains. The shift of a wavenumber to higher values reflects an increased number of gauche conformers in the acyl chains; i.e., the upward shift is a consequence of conformational disorder. These spectral parameters are considered to be diagnostic for the physical state of the lipid (Casal & Mantsch, 1984). Babin et al. (1987) observed that the wavenumber of the CH_2 stretching mode is temperature dependent even if the chain conformation remains unchanged. The observed slope of this variation is rather small, approximately 0.5 cm^{-1}/40 °C. These authors assumed that the value of the maximum intensity wavenumber can be taken as an indication for gauche/trans conformation. In Table II are summarized the major infrared absorption bands observed for solid ammonium salts of 1′- and 3′-DMPG and rac′-DMPG. Table III contains infrared wavenumbers observed in liposomes of 1′- and 3′-DMPG(NH_4^+) and 1′- and 3′-DMPG(Na^+).

The C–H stretching mode spectral region is very sensitive to the molecular order within the bilayer. The other characteristic acyl chain mode, CH_2 scissoring, gives rise to bands around 1470 cm^{-1}. The number of these bands as well as their exact wavenumber is dependent on the acyl chain packing and conformation (Casal & Mantsch, 1984). Other weak bands in the CH_2 scissoring region result from absorptions due to the polar headgroup and the terminal methyl groups. The deformation modes of terminal methyl groups occur at approximately 1460 cm^{-1} (asymmetric) and 1375 cm^{-1} (symmetric) (Amey & Chapman, 1983).

Figure 3A displays stacked contour plots of the CH_2 scissoring region of fully hydrated 1′-DMPG(NH_4^+) as a function of temperature in the region from 6 to 50 °C. The CH_2 scissoring gives rise to a single band at approximately 1467 cm^{-1}. 3′-DMPG(NH_4^+) reveals a similar behavior. Previously it has been found that the wavenumber of the methylene scissoring mode decreases with increasing temperature for liposomes of a pyrene-labeled phosphatidylcholine (Lotta et al., 1988). Similar low-wavenumber shift upon increasing temperature was observed for 1′- and 3′-DMPG(NH_4^+) (Table III) Cameron et al. (1980a) have shown that the CH_2 scissoring of DPPC in liposomes loses its intensity upon increasing temperature, which on the other hand is accompanied by an increase in the intensity of the shoulder peaks in the 1450–1440-cm^{-1} spectral region. This is typical behavior of the methylene scissoring mode upon melting of acyl chains (Nielsen & Hathaway, 1963; Snyder, 1967). Upon increasing temperature the infrared spectra of the CH_2 scissoring region of 1′- and 3′-DMPG(NH_4^+) reveal a shoulder band at 1457 cm^{-1} corresponding to the melting of the acyl chains (cf. Figure 3A).

(*b*) *Ester Carbonyl Stretching.* The carbonyl stretching vibration of the ester group is a useful infrared-active spectral region in the determination of the structural phase of membrane lipids (Casal & Mantsch, 1984; Lotta et al., 1988). It has been shown that the absorption bands in polycrystalline dipalmitoylphosphatidylcholine at 1739 and 1721 cm^{-1} are due

Table III: Compilation of the Infrared Absorption Bands (cm^{-1}) in the CH Stretching, CH_2 Scissoring, C=O Stretching, and the Polar Headgroup Region of 1′-DMPG(NH_4^+), 3′-DMPG(NH_4^+), 1′-DMPG(Na^+), and 3′-DMPG(Na^+)

	1′-DMPG(NH_4^+)		1′-DMPG(Na^+)		3′-DMPG(NH_4^+)		3′-DMPG(Na^+)	
assignment[a]	10 °C	40 °C	10 °C	40 °C	10 °C	40 °C	10 °C	40 °C
asym CH_3 stretch	2955	2956	2955	2955			2954	
asym CH_2 stretch	2917.0	2922.2	2917.6	2921.1	2917.8	2922.2	2918.4	2922.6
sym CH_3 stretch		2873	2874	2873				
sym CH_2 stretch	2850.1	2852.7	2850.3	2851.9	2850.1	2852.5	2850.4	2852.8
C=O stretch[b]	1734	1732	1739	1736	1734	1732	1735	1734
CH_2 scissoring	1467.4	1467.2	1467.6	1466.5	1467.5	1467.3	1473.3 1465.3	1467.3
asym PO_2^- stretch	1205	1209	1207	1214	1204	1200	1204	1206
asym C—O ester stretch	1171	1171	1172	1171	1172	1171	1172	1170
sym PO_2^- stretch	1087	1086	1089	1090	1087	1088	1099.6 1089.6	1090
sym C—O ester stretch	1067	1066	1067	1065	1068	1067	1074.6 1068	1068
C—OP stretch (phosphate ester stretch)	1047	1046	1049	1055	1050	1048	1051.6	1049

[a] See Amey and Chapman (1983), Casal and Mantsch (1984), and Casal et al. (1987c). [b] The wavenumber maximum of the broad C=O band contour.

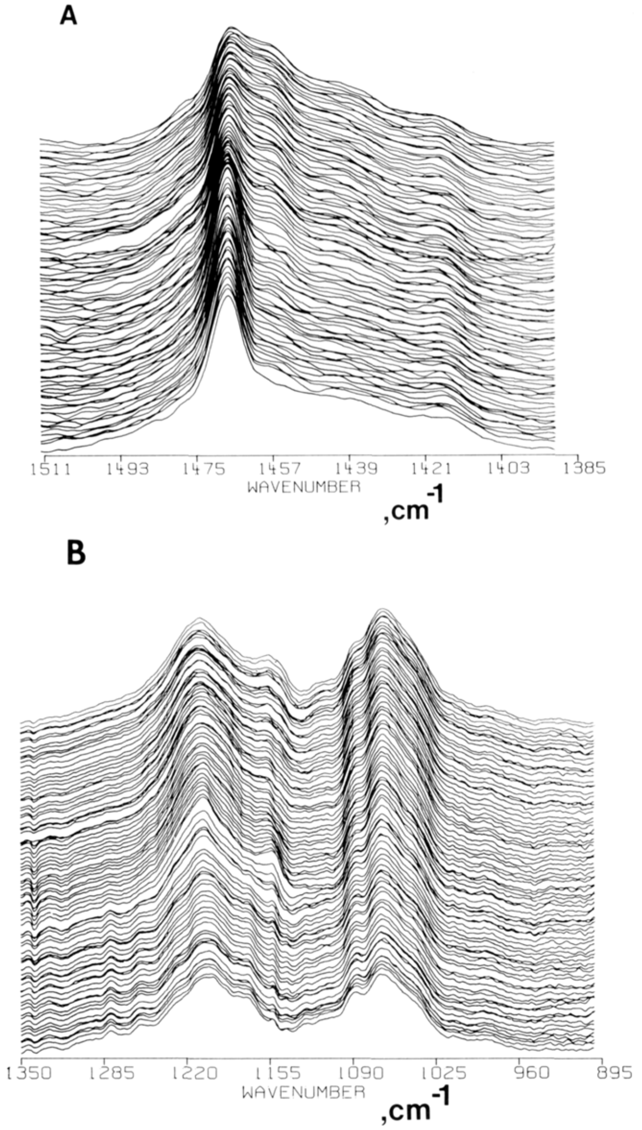

FIGURE 3: Stacked contour plots as a function of increasing temperature (6–50 °C, at 0.5 °C intervals from bottom to top) for fully hydrated 1′-DMPG as ammonium salt: (A) CH_2 scissoring; (B) 1350–800-cm^{-1} region.

to the C=O ester groups of the *sn*-1 and *sn*-2 acyl chains, respectively, thus suggesting conformational nonequivalence of the hydrocarbon chains. The wavenumbers ranging from about 1727 to 1744 cm^{-1} reflect a nearly complete trans conformation, while the wavenumbers between 1716 and 1728 cm^{-1} are characteristic of a gauche conformation of the C—C bond adjacent to the C=O group (Bush et al., 1980; Mushayakarara & Levin, 1982; Levin et al., 1982). However, in liposomes the two ester carbonyl bands due to the different conformations of the *sn*-1 (approximately 1742 cm^{-1}) and *sn*-2 (approximately 1725 cm^{-1}) C=O groups are usually seen only after resolution enhancement [Fourier self-deconvolution, see Casal and Mantsch (1984)].

Figure 4A shows the broad band contour of the C=O stretching mode of 1′-DMPG(NH_4^+) as a function of temperature. The position of the peak maximum shifts to lower wavenumbers upon increasing temperature (Table III). The half-bandwidths of the C=O bands were 39.5 and 40 cm^{-1} below and above T_m, respectively. For solid 1′-DMPG as an ammonium salt the half-bandwidth of the C=O stretching band was 31.6 cm^{-1}.

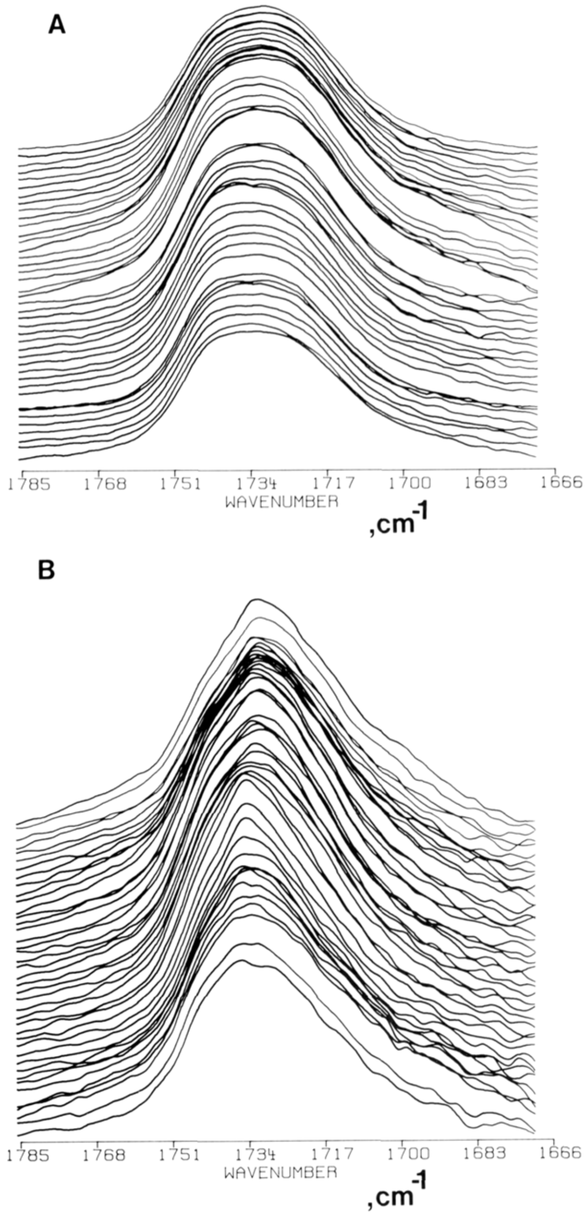

FIGURE 4: Infrared spectra of the C=O stretching region of 1′- and 3′-DMPG liposomes (ammonium salts) recorded at 1 °C intervals over the temperature range from 6 to 50 °C and shown from bottom to top in order of increasing temperature: (A) 1′-DMPG(NH_4^+); (B) 3′-DMPG(NH_4^+).

As mentioned above the C=O band can be resolved into components due to the *sn*-1 and *sn*-2 chain ester bonds. As the temperature increases, the relative peak heights of the two bands change. Using Fourier self-deconvolution technique (Lorentzian line 25 cm^{-1} wide and $K = 1.9$; Kauppinen et al., 1981), we resolved the carbonyl stretching band of 1′-DMPG(NH_4^+) into two components at approximately 1741 and 1725 cm^{-1} and assigned to the *sn*-1 and *sn*-2 carbonyl groups, respectively (not shown). The ratio of these components changes upon increasing temperature. At temperatures below the gel to liquid-crystalline transition the trans contribution is slightly dominated over the gauche conformation about the C—C bond adjacent to the C=O group; i.e., the higher wavenumber component at approximately 1741 cm^{-1} is more intense. At temperatures above the phase transition temperature the population of the ester linkages possessing gauche conformation about the C—C bond adjacent to the C=O group increases, reflecting a more disordered state. The ratio $I_{1741\mathrm{cm}^{-1}}/I_{1725\mathrm{cm}^{-1}}$ of the relative intensities of the bands is about 1.3 at 10 °C and about 1.2 at 40 °C. Although the change in ratio of the relative intensities is small, there is an abrupt discontinuity at the phase transition at approximately 21 °C.

In Figure 4B is shown the ester carbonyl stretching mode of 3′-DMPG(NH_4^+) in the 6–50 °C temperature range. The peak position of the broad band of 3′-DMPG(NH_4^+) also reveals a lower wavenumber shift at approximately 21 °C, corresponding to the gel to liquid-crystalline phase transition. The bandwidth of the broad C=O stretching mode is about 40 cm^{-1} both below and above T_m and equals the half-bandwidth observed for 1′-DMPG(NH_4^+). In the solid phase the C=O stretching band appears at 1739.5 cm^{-1} with a half-bandwidth of 29 cm^{-1}. Self-deconvolution of this band revealed two components at approximately 1740 and 1727 cm^{-1} due to the *sn*-1 and *sn*-2 acyl chains, respectively (Lorentzian line 25 cm^{-1} wide and $K = 2.1$ were used for the Fourier self-deconvolution). The $I_{1740cm^{-1}}/I_{1727cm^{-1}}$ was 1.3 at temperatures below the gel to liquid-crystalline phase transition (characteristic of trans conformation), whereas above T_m the gauche conformation is dominating.

(*c*) *Phosphate Group Region.* The most dominant features in the 1350–800-cm^{-1} region are due to the vibrations of the phosphate moiety. The asymmetric and symmetric stretching modes of PO_2^- appear typically at 1240–1220 and 1090 cm^{-1}, respectively (Casal et al., 1987a). The wavenumber of this mode is sensitive to the hydration of the phosphate group, revealing values around 1220 cm^{-1} for hydrated and 1235–1250 cm^{-1} for dehydrated phosphate groups (Casal et al., 1987a). Because of the overlapping modes it is not straightforward to examine the thermotropic behavior of this spectral region. On the other hand, transition from the gel to liquid-crystalline phase induces practically no changes in these modes (Casal & Mantsch, 1984). Casal et al. (1987c) have shown that for anhydrous samples this spectral region is sensitive to interactions with metal ions. In the gel phase of phospholipid liposomes also the methylene wagging band progression features are evident. A progression of eight weak and regularly spaced bands at about 1200, 1220, 1245, 1265, 1290, 1310, and 1345 cm^{-1} are generally observed (Casal & Mantsch, 1984; Cameron et al., 1980a). These bands are absent in the liquid-crystalline phase. In the gel phase upon decreasing the temperature the bands assigned to the CH_2 wagging band progression increase considerably in intensity (Cameron et al., 1980a). The band progression results from the wagging of several coupled CH_2 oscillators in an all-trans conformation (Snyder & Schachtschneider, 1963). The observed wavenumber pattern is specific to the length of the all-trans segment of the chain (Cameron et al., 1980a). Unfortunately, the CH_2 wagging progression is superimposed with the asymmetric PO_2^- band. There is also the CH_2 rocking band progression in the 1150–700-cm^{-1} region. However, these bands are even weaker than those due to the CH_2 wagging progression (Casal & Mantsch, 1984).

Stacked contour plots in the 1350–800-cm^{-1} region for 1′-DMPG(NH_4^+) liposomes are displayed as a function of temperature in Figure 3B and reveal no drastic changes. For 1′-DMPG(NH_4^+) the PO_2^- asymmetric stretching mode appears at about 1205 cm^{-1} and is slightly shifted toward higher wavenumbers upon increasing temperature. The asymmetric ester C–O stretching band arises as a shoulder at approximately 1171 cm^{-1} (Casal & Mantsch, 1984). The two other major bands in the 1350–800-cm^{-1} region are assigned to the symmetric PO_2^- stretching at approximately 1087 cm^{-1} and to the symmetric ester C–O stretching mode at approximately 1067 cm^{-1} with a shoulder at approximately 1047 cm^{-1} assigned to the phosphate ester stretch (C–OP stretch) (Casal & Mantsch, 1984; Casal et al., 1987c) (cf. also Tables II and III). In addition, a series of very weak bands arising from the progression in CH_2 wagging (in the 1350–1200-cm^{-1} region) were observed below T_m (21 °C). At higher temperatures, the coupling between similar vibrations along a sequence of unit cells is disrupted upon gauche rotamer formation. Because of low intensity, however, even in the gel phase the 1000–800-cm^{-1} region does not reveal bands due to the CH_2 rocking band progression.

The spectral features of 3′-DMPG(NH_4^+) in the 1350–800-cm^{-1} region as a function of temperature are very similar to those of 1′-DMPG(NH_4^+) (cf. Tables II and III). The band pattern is similar to the spectra for other phospholipids in aqueous media (Casal & Mantsch, 1984; Casal et al., 1987a) and has been associated with the phosphate group being in the gauche-gauche conformation. The gauche-gauche conformation is commonly found in the single-crystal structures of phosphate diesters (Casal et al., 1987c). In addition, the infrared spectra of solid 1′- and 3′-DMPG as ammonium salts resemble those of 1′- and 3′-DMPG(NH_4^+) liposomes. Upon increasing temperature the asymmetric PO_2^- stretching mode of 3′-DMPG(NH_4^+) first shows a small low-wavenumber shift at $T_m = 21$ °C and then shifts slightly to higher wavenumbers. Below T_m the band pattern associated with the CH_2 wagging band progression is evident. The 1000–800-cm^{-1} region does not show the CH_2 rocking band progression.

Comparison of the Infrared Spectra of 1′-DMPG(Na⁺) and 3′-DMPG(Na⁺). (*a*) *Acyl Chain Bands.* The presence of 300 mM NaCl causes the transition temperature of 1′-DMPG to increase from 21 to 23 °C (Figure 2A), suggesting tighter packing of the acyl chains. Below the phase transition 300 mM NaCl does not significantly affect the acyl chain conformation. It appears that there is less conformational disorder in 1′-DMPG(Na^+) in the liquid-crystalline phase because of the minor wavenumber shift observed for 1′-DMPG(Na^+); i.e., the final liquid-crystalline phases of 1′-DMPG(NH_4^+) and 1′-DMPG(Na^+) differ somewhat from each other (Figure 2A).

Significantly higher temperature is required to melt the 3′-DMPG(Na^+) complex (Figure 2B). This suggests that the complexing of 3′-DMPG with Na^+ induces crystallization of the acyl chains. The more ordered, highly crystalline phase involves a phase transition to liquid-crystalline phase at 33 °C ($=T_{hc}$). There is a minor increase in the wavenumber of 3′-DMPG(Na^+) at approximately 20–23 °C. This probably reflects the "free" 3′-DMPG (Casal et al., 1987c; cf. also Figure 1D). At temperatures below 21 °C the conformational order (the ratio of trans/gauche bonds in the acyl chains) of the gel phase of 3′-DMPG(NH_4^+) and the highly crystalline phase of 3′-DMPG(Na^+) is similar at 10 °C. The symmetric methylene stretching modes of 3′-DMPG(NH_4^+) and 3′-DMPG(Na^+) were observed at 2850.1 and 2850.4 cm^{-1}, respectively. Furthermore, the symmetric stretching wavenumbers measured at 40 °C were found at 2852.5 and 2852.8, respectively. Accordingly, the final liquid-crystalline phases of 3′-DMPG(NH_4^+) and 3′-DMPG(Na^+) are similar (Figure 2B). The half-bandwidths of the symmetric stretching mode of 1′- and 3′-DMPG(Na^+) are equal to those for 1′- and 3′-DMPG(NH_4^+), respectively, both below and above the phase transition temperature.

Figure 5A shows the CH_2 scissoring of 1′-DMPG(Na^+) as a function of temperature in the region from 6 to 50 °C. Similarly to 1′-DMPG(NH_4^+) 1′-DMPG(Na^+) also reveals a single band at approximately 1467 cm^{-1}. The wavenumber of the methylene scissoring mode decreases with increasing temperature (Table III). Upon increasing temperature the

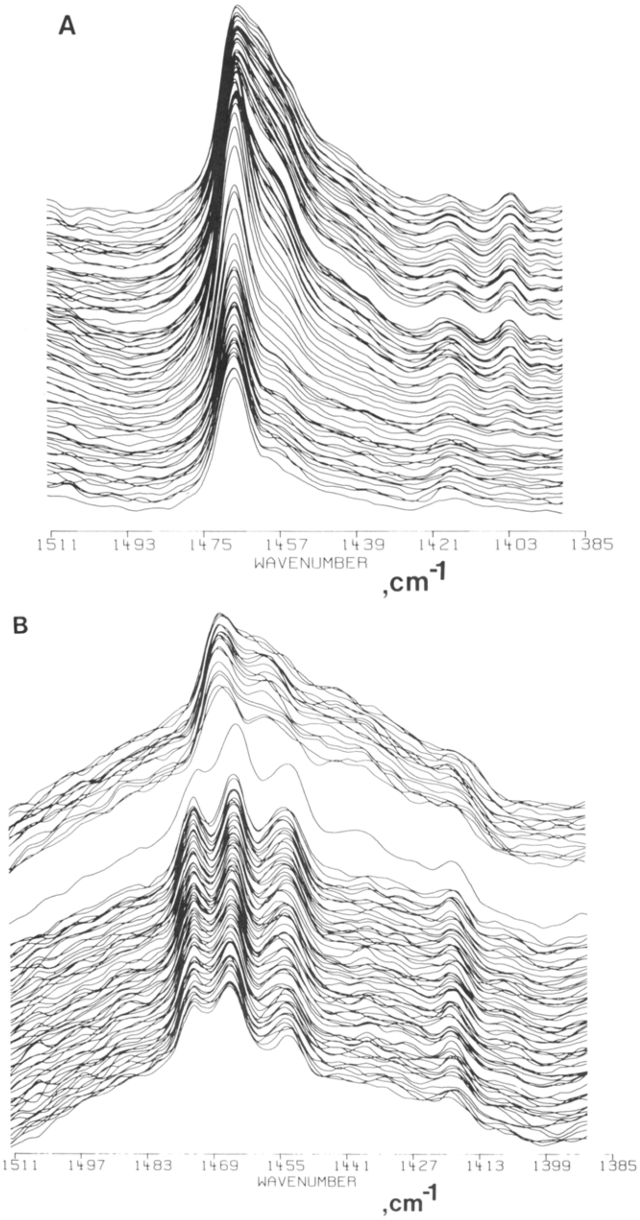

FIGURE 5: Stacked contour plots of the CH_2 scissoring region as a function of increasing temperature (at 0.5 °C intervals from bottom to top) for fully hydrated 1′- and 3′-DMPG hydrated in buffer containing 300 mM NaCl: (A) 1′-DMPG(Na^+) (6–50 °C); (B) 3′-DMPG(Na^+) (6–40 °C).

CH_2 scissoring region of 1′-DMPG(Na^+) also involves a shoulder peak at 1457 cm^{-1} (Figure 5A). The behavior of the CH_2 scissoring mode of 1′-DMPG(Na^+) upon increasing temperature is thus similar to that observed for 1′-DMPG(NH_4^+).

In Figure 5B is shown the methylene scissoring region of 3′-DMPG(Na^+) in the temperature range 6–40 °C. At temperatures below approximately 33 °C the infrared spectrum of the CH_2 scissoring of 3′-DMPG(Na^+) differs significantly from that observed in the absence of Na^+. This temperature represents the melting of the highly crystalline phase formed in the presence of 300 mM NaCl (cf. Table I). At 10 °C the CH_2 scissoring of 3′-DMPG(Na^+) consists of three bands at 1473.3, 1465.3, and 1453.5 cm^{-1}. The first two wavenumbers are assigned to CH_2 scissoring modes, and the latter, weaker one is assigned to asymmetric terminal methyl bending (Amey & Chapman, 1983). At 40 °C, i.e., above the temperature of the transition from highly crystalline to liquid-crystalline phase, the CH_2 scissoring region is dominated by a single strong band at 1467.3 cm^{-1} with a shoulder at approximately 1458 cm^{-1}.

The overall thermotropic behavior and the shape of the CH_2 scissoring band contour of 3′-DMPG(Na^+) observed at temperatures above 33 °C show characteristics similar to those of 3′-DMPG(NH_4^+) and 1′-DMPG. The band at approximately 1454 cm^{-1} in the highly crystalline phase assigned to the asymmetric bending of methyl groups is so weak in intensity that at temperature above 33 °C it is impossible to detect. The peak intensities decrease and the bandwidths widen because of an increased degree of conformational disorder introduced during the order–disorder phase transition. A shoulder peak appears at approximately 1457 cm^{-1} upon increasing temperature. It is likely that the very weak asymmetric CH_3 bending mode that widens in half-bandwidth and decreases in intensity with increasing temperature is superimposed with the shoulder of the CH_2 scissoring mode at higher temperatures (Figure 5B).

(*b*) *Ester Carbonyl Stretching.* Figure 6A displays the C=O stretching mode of 1′-DMPG(Na^+) at different temperatures. The half-bandwidth was approximately 34 and 35 cm^{-1} below and above the phase transition at 23 °C, respectively. The decreased bandwidths compared to 1′-DMPG(NH_4^+) indicate slightly decreased motional freedom in the interfacial region in the presence of 300 mM NaCl. The decreased bandwidths for 1′-DMPG(Na^+) are in accordance with the assumption of somewhat tighter packing of the acyl chains. The broad band contour of 1′-DMPG(Na^+) shows a slight shift to lower wavenumbers at approximately 23 °C, corresponding to the main transition.

The peak position of the C=O stretching mode shows a more drastic shift toward lower wavenumbers in the temperature interval of 34–40 °C. Yet a temperature scan of the CH_2 symmetric stretching mode of 1′-DMPG(Na^+) does not reveal discontinuities indicative of structural rearrangements. Resolution enhancement (Lorentzian line 25 cm^{-1} wide and $K = 2.2$ were used for self-deconvolution) induces the C=O stretching band of 1′-DMPG(Na^+) to separate into at least two components at approximately 1741 and 1724 cm^{-1}. In the self-deconvoluted spectra above 40 °C the observed wavenumber values are 1746 (a shoulder), 1736, and 1719 cm^{-1}. The relative ratio ($I_{1741\text{cm}^{-1}}/I_{1724\text{cm}^{-1}}$) is ≈2.1 below T_m (at 23 °C), pointing out that the population of the gauche conformation about the C—C bond adjacent to the C=O group is minor. In the temperature range 23–35 °C a value of 1.8 was measured, indicating a somewhat increasing gauche contribution. However, only at temperatures above 40 °C is the population of the C—C gauche conformation about the C—C bonds adjacent to the ester carbonyl significant, as indicated by the value of 1.5 for the ratio $I_{1736\text{cm}^{-1}}/I_{1719\text{cm}^{-1}}$.

Because the structural rearrangement observed at higher temperatures ($T > 40$°C) in the interface region of 1′-DMPG(Na^+) is not accompanied by changes in the acyl chain region, it is reasonable to suggest that structural alterations are restricted to the polar headgroup region of 1′-DMPG(Na^+).

The stacked contour plots of the C=O stretching region displayed for 3′-DMPG(Na^+) in Figure 6B differ significantly from those presented for 1′-DMPG(NH_4^+), 3′-DMPG(NH_4^+), and 1′-DMPG(Na^+). In the highly crystalline phase of 3′-DMPG(Na^+) the half-bandwidth of the C=O stretching mode is about half that observed for the other complexes. The bandwidth is approximately 19 cm^{-1} below 33 °C. Upon increasing temperature it increases with a drastic change at T_{hc} (highly crystalline to liquid-crystalline transition). The

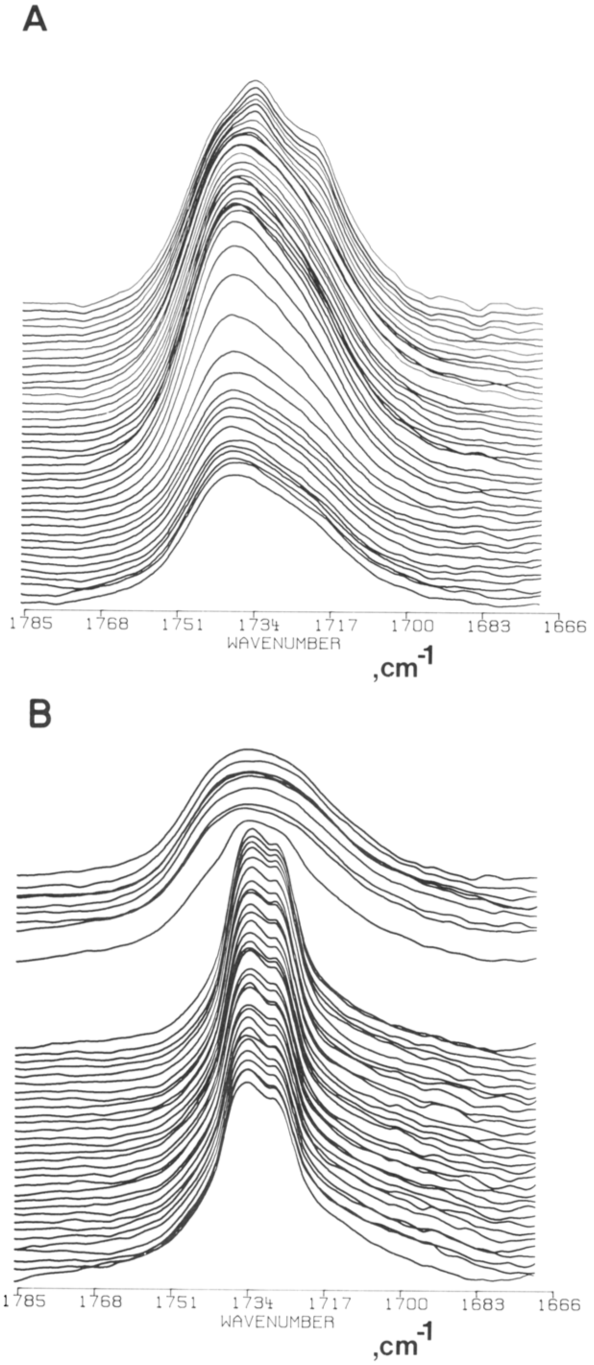

FIGURE 6: Infrared spectra of the C=O stretching region recorded at 1 °C intervals and plotted from bottom to top in order of increasing temperature: (A) 1′-DMPG(Na^+) (6–50 °C); (B) 3′-DMPG(Na^+) (6–40 °C).

bandwidth is about 40 cm^{-1} above the transition. This band narrowing suggests that Na^+ binds tightly to 3′-DMPG, leading to the immobilization of the entire phospholipid polar headgroup.

In the highly crystalline phase the C=O stretching of 3′-DMPG(Na^+) is composed of at least two components at 1735 and 1728 cm^{-1}. We have also applied self-deconvolution technique (Lorentzian lines of 8 cm^{-1} full width at half-height and resolution enhancement factor $K = 1.7$). In the deconvoluted spectrum of 3′-DMPG(Na^+) at temperatures below 33 °C there are two main bands at 1735 and 1727 cm^{-1} and a clearly separable shoulder at 1745 cm^{-1}. The relative ratio of $I_{1735\text{cm}^{-1}}/I_{1727\text{cm}^{-1}}$ was 1.2; i.e., the population of trans and gauche conformation about the C—C bonds adjacent the C=O groups should be nearly equivalent. The peak at 1745 cm^{-1} is suggested to be due to crystal effects. The interaction of Na^+ with 3′-DMPG has more profound effects than simply restricting the motional freedom of acyl chains. At the level of the ester C=O group the effect by Na^+ involves immobilization, which further causes site-symmetry splitting. Similar behavior has been found for DMPS–Li^+ complexes (Casal et al., 1987a). When the ester carbonyl groups in the interface region of phospholipids form strong hydrogen bonds, the wavenumber of the C=O stretching mode is below 1715 cm^{-1} (Levin, 1984). In the DMPS–Ca^{2+} complex one of the ester carbonyl groups is engaged in hydrogen bonding (Casal et al., 1987a). Neither 1′- nor 3′-DMPG, both in the absence and in the presence of NaCl, reveals bands associated with a hydrogen-bonded ester C=O stretch.

(*c*) *Phosphate Group Region.* The band contours of 1′-DMPG(NH_4^+) and 1′-DMPG(Na^+) show similar behavior in both the gel and liquid-crystalline phase (below 40 °C), indicating that the conformation of the phosphate group is gauche-gauche (Casal et al., 1987a–c). However, upon increasing temperature the shoulder bands of 1′-DMPG(Na^+) at approximately 1055 (assigned to the phosphate ester stretch) and at 1040 cm^{-1} increase, and the wavenumber of the band assigned to the symmetric ester C–O mode reveals a low wavenumber shift. In addition, the asymmetric PO_2^- stretching mode appears at approximately 1220 cm^{-1} involving a high-wavenumber shift (Figure 7A). These changes can be connected to those found in the interfacial region of 1′-DMPG(Na^+) at temperatures above 40 °C and are associated with rearrangements in the polar headgroup. However, the conformation of the two P–O ester bands remains gauche–gauche. The Na^+ binding probably only induces a conformational change in the glycerol backbone of 1′-DMPG (Casal et al., 1987a–c). Below the main transition temperature at 23 °C the bands belonging to the CH_2 wagging band progression of 1′-DMPG(Na^+) are evident. No bands assigned to the methylene rocking band progression were observed in the 1000–800-cm^{-1} region.

In the 1350–800-cm^{-1} region the stacked contour plots of 3′-DMPG(Na^+) differ significantly from those for 1′-DMPG(NH_4^+) and 1′-DMPG(Na^+), as well as from those of 3′-DMPG(NH_4^+) when the latter are in the ordered phase (Figure 7B). For 3′-DMPG(Na^+) a very complicated spectral structure is observed in the highly crystalline phase at temperatures below 33 °C. In the 1350–1200-cm^{-1} region several narrow regularly spaced CH_2 wagging band progressions are seen. The bands at 1227, 1237, 1257, 1290, 1329, and 1344 cm^{-1} arise from a progression in the CH_2 wagging mode. These bands are quite intensive over the entire highly crystalline phase. In addition, band pattern at wavenumbers of 986, 929, 885, and 814 cm^{-1} is observed in the 1000–800-cm^{-1} range arising from a progression in the CH_2 rocking. The appearance of this peak pattern indicates that the coupling between similar vibrations along a sequence of unit cells is strong, in accordance with the data describing the packing of the hydrocarbon chains (see below). The infrared absorption bands of 3′-DMPG(Na^+) in the 1350–800-cm^{-1} region are summarized in Table III.

The pronounced band narrowing and splitting observed for the 1350–800-cm^{-1} spectral region upon Na^+ binding indicates reduction in the motional freedom of the polar headgroup. In the highly crystalline phase the spectra of 3′-DMPG(Na^+) show a pattern of bands compatible with the phosphate group being in the gauche-gauche conformation (Casal et al., 1987a–c). However, a conformational change in the glycerol backbone is also evident. For several PS it has been found

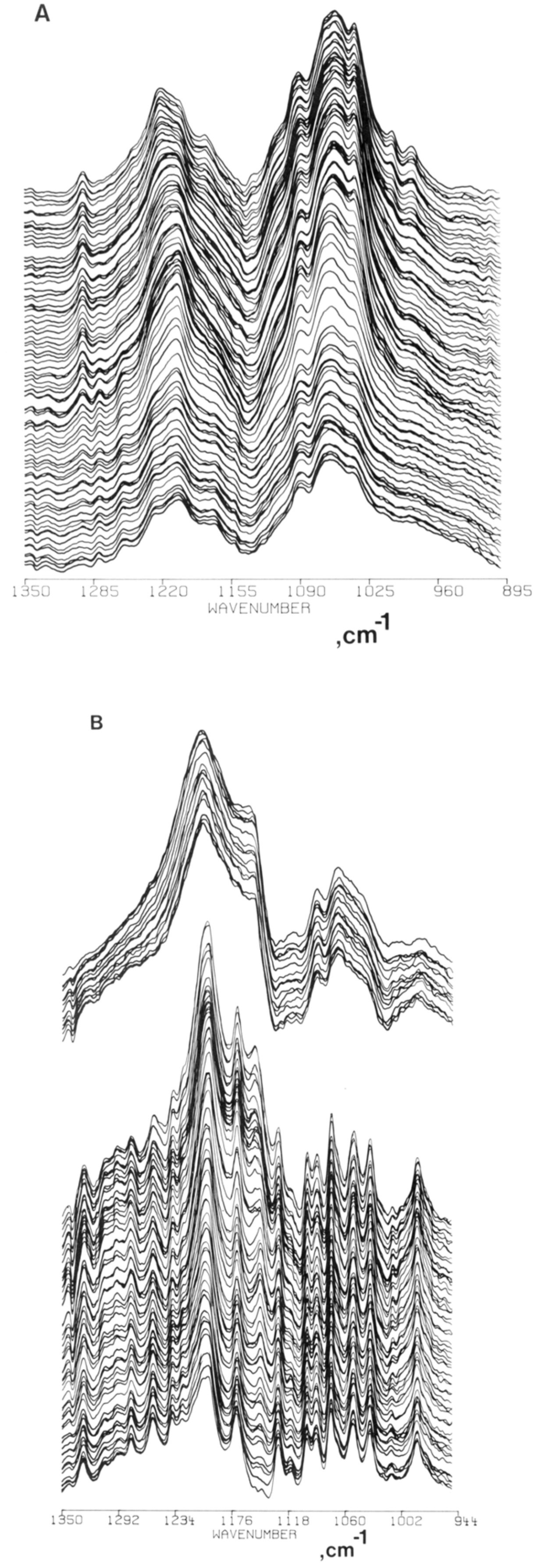

FIGURE 7: Stacked contour plots (at 0.5 °C intervals) of the infrared spectra of fully hydrated 1′-DMPG and 3′-DMPG liposomes in the 1350–800-cm^{-1} region shown from bottom to top in order of increasing temperature: (A) 1′-DMPG(Na$^+$) (6–50 °C); (B) 3′-DMPG(Na$^+$) (6–40 °C).

that the binding of Ca^{2+} results in a conformational change in the P–O ester bonds from gauche-gauche to antiplanar-antiplanar (Casal et al., 1987a–c).

At temperatures greater than T_{hc} the spectral features of 3′-DMPG(Na$^+$) are similar to those for 3′-DMPG(NH$_4^+$). Disappearance of band progression is evident, and the bands are broadened, thus indicating increased motional freedom. The asymmetric PO$_2^-$ stretching mode at approximately 1206 cm^{-1} shows a shift to higher wavenumbers (Figure 7B and Table III).

Complexes of DMPS with Li$^+$ and Ca^{2+} reveal a more ordered lipid phase, and it has been shown that the cations bind to the phosphate moiety, causing removal of water from the hydration shell (Casal et al., 1987a). There is a shift in the wavenumber of the asymmetric PO$_2^-$ stretching mode from 1200 to 1230 cm^{-1}, indicating the loss of bound water from the DMPS phosphate group. In the spectrum of DMPS–Ca^{2+} the asymmetric PO$_2^-$ stretching is at 1240 cm^{-1}, typically to a dehydrated phosphate group (Casal et al., 1987a). For 3′-DMPG(Na$^+$) the degree of hydration of the phosphate moiety is not so clear on the basis of infrared data alone, because in the highly crystalline phase the asymmetric PO$_2^-$ stretching mode appears at approximately 1204 cm^{-1} and the corresponding band of solid anhydrous 3′-DMPG as an NH$_4^+$ salt on KBr pellet was observed at 1205 cm^{-1} (Table II). However, the data dealing with the interaction of Na$^+$ with 3′-DMPG indicate a key role of the polar headgroup in the complex formation. As documented in several reports, the chain crystallization is a consequence of the ions interacting with the lipid headgroups (Casal et al., 1987c).

Acyl Chain Packing. The splitting due to a crystal field effect has been previously observed in the spectra of *n*-alkanes, terminally substituted *n*-alkanes, and polyethylenes (Snyder, 1961, 1979; Casal et al., 1982, 1983), fatty acids (Koyama et al., 1977), and anhydrous films of DPPC (Fookson & Wallach, 1978). Cameron et al. (1980a,b) have found that the splitting of the CH$_2$ scissoring mode below the pretransition temperature is characteristic to this structural alteration. Temperature dependences of the crystal field splitting of the methylene scissoring bands of a series of fully hydrated gel-phase diacyl phospholipids were determined (Cameron et al., 1981). Recently it was shown that the CH$_2$ scissoring of DMPS–Li$^+$ and DMPS–Ca^{2+} complexes is split into two components by the crystal field (Dluhy et al., 1983).

The crystal field splitting observed in the CH$_2$ scissoring mode does not occur in the hexagonal or triclinic subcells but is specific to orthorhombic or monoclinic crystal lattice unit cell, both of which have an orthorhombic subcell (Snyder, 1979). On the other hand, a single CH$_2$ scissoring mode indicates hexagonal or triclinic packing, reflecting significant reorientational fluctuations of the acyl chains. In the hexagonal type of packing the intermolecular interactions are minimized and the acyl chains are generally viewed as behaving like rigid rotors independently of each other. Below the pretransition the infrared spectra of DPPC liposomes consist of a single CH$_2$ scissoring band, and according to the X-ray and Raman data hexagonal packing is preferred over triclinic (Cameron et al., 1980a,b). However, orthorhombic or monoclinic unit cells are similar, and therefore the exact crystal lattice cannot be directly determined from the infrared data (Snyder, 1979). A detailed analysis of the intermolecular interaction has been carried out on the basis of atom–atom potentials (Snyder, 1961; Tasumi & Shimanouchi, 1965).

The magnitude of band separation characterizes the degree of interchain interaction, i.e., interchain vibrational coupling

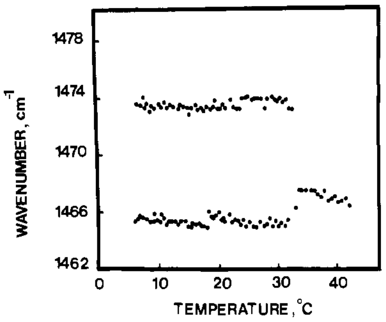

FIGURE 8: Crystal field induced splitting of the CH_2 scissoring mode of 3′-DMPG(Na^+) as a function of temperature.

(Decius & Hexter, 1977), a larger splitting suggesting a tighter packing of the fatty acid chains accompanied by a decrease in the amplitudes and rates of motion around the long axes of the hydrocarbon chains. As discussed by Cameron et al. (1981), the magnitude of crystal field splitting at any given temperature depends on two factors. First, a dynamic factor reflects the degree of torsional and librational motion about the long axis of the acyl chains. The effect of the dynamic factor is well demonstrated for DPPC (Cameron et al., 1980a). The splitting of the CH_2 scissoring mode introduced at the pretransition increases progressively in magnitude with decreasing temperature, and at approximately −60 °C the CH_2 scissoring mode splits by about 10 cm^{-1} (Cameron et al., 1980a). The reduction of the splitting with increasing temperature implies loosening of acyl chain packing. This involves an increased rotational motion of the acyl chains in the orthorhombic subcell yet without loss of the subcell shape (Cameron et al., 1980a). The other, static factor reflects the interchain distance and the degree to which the hydrocarbon chains can pack in the orthorhombic subcell. In general, the wavenumber separation will decrease with an increase in interchain distances. In *n*-alkanes the effect of the static factor is minimized, and a uniform packing with strong van der Waals interactions is evident. In phospholipids the interchain interaction will be greatest in the central region of the acyl chains which most closely resembles the *n*-alkanes.

There are several factors affecting the interchain interactions and via that the packing of the acyl chains: introduction of progressively larger terminal groups, reduction of the acyl chain length, and the cross-sectional area of the headgroup (Cameron et al., 1980a). Very recently, we have reported on the lack of the pretransition for PPDPC liposomes (Lotta et al., 1988). The introduction of pyrene moiety as the terminal group of the *sn*-2 acyl chain reduces interchain vibrational coupling, leading to the disappearance of the pretransition. Finally, at lower temperatures where the dynamic effects are minimal, the observed band splittings induced by the crystal field are most prominent, as shown for DPPC (Cameron et al., 1980a,b).

When comparing the spectral features arising from the CH_2 scissoring modes of fully hydrated 1′-DMPG(NH_4^+) as well as 1′- and 3′-DMPG(Na^+) shown in Figures 3A and 5, one observes that the spectral structures of 3′-DMPG(Na^+) in the highly crystalline phase differ significantly from those of the other lipid samples. In the infrared spectrum of the CH_2 scissoring band of 3′-DMPG(Na^+) the appearance of splitting of the mode into bands at approximately 1473 and 1465 cm^{-1} is evident. Temperature-independent crystal field splitting of the CH_2 scissoring mode of 3′-DMPG(Na^+) is shown in Figure 8.

As was discussed above, this band pattern in the CH_2 scissoring region is compatible with the fatty acyl chains of 3′-DMPG(Na^+) being packed below 33 °C in an orthorhombic-like subcell in an orthorhombic or monoclinic crystal lattice. In contrast, in the liquid-crystalline phase the infrared spectra of the CH_2 scissoring mode of 3′-DMPG(Na^+) are characteristic to the hexagonal acyl chain packing (Figure 5B). As an ammonium salt 3′-DMPG also packs in a hexagonal lattice over the temperature region 6–50 °C (not shown).

The crystal field induced splitting of the CH_2 scissoring band of 3′-DMPG(Na^+) in the highly crystalline phase below 33 °C was approximately 8 cm^{-1}. Importantly, the splitting is temperature independent from 6 to 33 °C (Figure 8); i.e., even at relatively high temperatures rigid packing with reduced amplitudes and reduced rates of torsional and librational motion about the long axis of the acyl chains is evident. Thus, the effect of the dynamic factor is minimal on the crystal field splitting, and the chain coupling is dominated by the static factor. On the other hand, the effect of the static factor is minimized when the potential associated with steric effects reducing the intermolecular interaction has its minimum. Both 3′-DMPG(NH_4^+) and 3′-DMPG(Na^+) are sterically equal in the acyl chain region. Accordingly, the dominating contribution to the crystallization comes from the organization at the headgroup level. A reasonable assumption is that the complexation of 3′-DMPG with Na^+ reduces the cross-sectional area of the headgroup and minimizes interactions in the interface region and thus allows tighter packing of the acyl chains. This is also indicated by the demonstrated significantly higher affinity of Na^+ for 3′-DMPG than for the *sn*-1′ stereoisomer (Eklund et al., 1987). This difference was interpreted to be due to a slightly different favored conformation of the headgroup moiety in the 3′ stereoisomer. In addition, for 1′-DMPG(NH_4^+) and 1′-DMPG(Na^+) the observed wavenumbers and the fact that the CH_2 scissoring mode reveals only a single band indicate the packing of the fatty acid acyl chains to be hexagonal in the temperature region 6–50 °C (Figures 3A and 5A).

The observed more ordered lipid phase of DMPS–Li^+ also involves an orthorhombic subcell packing of the acyl chains and reveals a crystal field splitting in the CH_2 scissoring mode by approximately 12 cm^{-1}. In the presence of Ca^{2+} the splitting is about 7 cm^{-1} (Casal et al., 1987a). The tight packing of the hydrocarbon chains in 3′-DMPG(Na^+) is intermediate between DMPS–Li^+ and DMPS–Ca^{2+}. The gel phases of fully hydrated Na^+ and NH_4^+ salts of DMPS, however, yield an infrared spectra typical of systems with acyl chains packed in a hexagonal lattice (Casal et al., 1987a).

One central problem in the packing of the phospholipids in bilayers concerns whether or not the hydrocarbon chains are interdigitated. The interchain interactions are likely to be significantly enhanced in fully interdigitated lipid bilayers. Siminovitch et al. (1987) have proposed how to estimate the degree of interdigitation. Accordingly, the pressure-induced crystal field splitting of the methylene scissoring and rocking modes should provide indications of chain interdigitation (Siminovitch et al., 1987). Qualitatively, even the features of the bandshapes (of, for instance, the CH_2 scissoring region displayed in stacked contour plots) can be used to distinguish between interdigitated and noninterdigitated organizates. For interdigitated bilayers the splitting of the CH_2 scissoring into two well-defined bands at higher pressures is more abrupt and immediately apparent in the stacked contour plots. On the other hand, in noninterdigitated bilayers a broad shoulder on the low-wavenumber side of the CH_2 scissoring band is first observed. This shoulder gains steadily in intensity until a well-defined crystal field component band of CH_2 scissoring becomes apparent (Siminovitch et al., 1987).

The spectral features in stacked contour plots of the CH_2 scissoring region of 3′-DMPG(Na^+) resemble those found for interdigitated systems (Figure 5B). Finally, in the infrared spectra of the highly crystalline lipid phase of 3′-DMPG(Na^+) the vibrational mode assigned to the asymmetric terminal methyl mode is observed at approximately 1454 cm^{-1} (Figure 5B). The wavenumber of this mode remains constant in the highly crystalline phase (6–33 °C), and the bandwidth of the asymmetric CH_3 bending mode decreases when compared to the spectra recorded above 33 °C. This indicates reduced rotational motion of the terminal group in the highly crystalline phase; i.e., the end groups of the acyl chains are immobilized. These two findings may be taken as evidence for hydrocarbon chain interdigitation in the highly crystalline phase of 3′-DMPG(Na^+).

CONCLUSIONS

The results from the infrared measurements reported here supplement our DSC data on the structure and dynamics of Na^+–DMPG interactions. To determine the ion–lipid interactions on a molecular level, the CH_2 stretching and scissoring modes, the C=O stretching mode, and the 1350–800-cm^{-1} region of the phospholipid infrared spectrum were monitored in detail.

After a prolonged incubation the thermotropic phase behaviors of 1′-DMPG(Na^+) and 3′-DMPG(Na^+) differ significantly from each other. For 3′-DMPG complexation with Na^+ causes the appearance of a more ordered, highly crystalline phase, which has a transition into the liquid-crystalline phase at significantly higher temperatures (at 33 °C) than 1′- or 3′-DMPG(NH_4^+) (at 21 °C) or 1′-DMPG(Na^+) (at 23 °C) have T_m. In this highly crystalline phase the infrared spectra of the 3′-DMPG(Na^+) complex are compatible with the hydrocarbon chains being packed in an orthorhombic- or monoclinic-like crystal lattice. This is indicated by the crystal field splitting of the CH_2 scissoring mode resulting from the interchain vibrational coupling of adjacent acyl chains. The splitting of the methylene scissoring mode is temperature independent, suggesting lack of involvement of the dynamic factor in the splitting. This demonstrates a rigid packing of the lipid in the highly crystalline phase with reduced amplitudes of both torsional and librational motions about the long axis of the acyl chains. In addition, the terminal methyl end groups of the acyl chains are immobilized in the highly crystalline phase, perhaps reflecting hydrocarbon chain interdigitation. In contrast, both the gel and liquid-crystalline phases of 1′-DMPG(NH_4^+), 3′-DMPG(NH_4^+), and 1′-DMPG(Na^+) and the liquid-crystalline phase of 3′-DMPG(Na^+) are characterized by packing of the hydrocarbon chains in a hexagonal lattice, consistent with the appearance of a single band in the CH_2 scissoring region.

The temperature independence of the crystal field splitting observed in the CH_2 scissoring region of 3′-DMPG(Na^+) reveals the involvement of strong intermolecular interactions and further signifies the importance of the static factor in interpreting the acyl chain packing of 3′-DMPG(Na^+). On the other hand, the effect of the static factor is minimized when the potential associated with repulsive steric effects has its minimum. For 3′-DMPG(NH_4^+) and 3′-DMPG(Na^+) the hydrocarbon chain regions are sterically equal. Accordingly, the organization of the polar headgroup plays an important role in formation of the highly crystalline 3′-DMPG(Na^+). In the infrared spectrum of 3′-DMPG(Na^+) the interaction between cation and lipid causes very fine spectral structure with narrow bands. Even the methylene band wagging and rocking progression patterns are seen in the 1350–800-cm^{-1} region. In the highly crystalline phase also the bandwidth of the C=O stretching mode is reduced. This kind of band narrowing is associated with reduction in motional freedom and demonstrates that Na^+ bings tightly to the 3′-DMPG polar headgroup, thus leading to a phase with an efficient immobilization of the polar headgroup. However, it is evident that the phosphate group remains in the gauche-gauche conformation for both 1′- and 3′-DMPG, and Na^+ induces structural changes in the glycerol backbone.

ACKNOWLEDGMENTS

We express our gratitude to Sirpa Turtiainen for technical assistance and for the processing of the infrared data. We thank Dr. Hector L. Casal (National Research Council of Canada, Ottawa, Canada) for sending us several preprints of his manuscripts.

Registry No. 1′-DMPG, 57618-28-7; 3′-DMPG, 110797-69-8; Na, 7440-23-5.

REFERENCES

Amey, R. L., & Chapman, D. (1983) in *Biomembrane Structure and Function. Topics Molecular and Structural Biology* (Chapman, D., Ed.) Vol. 4, pp 199–256, MacMillan, London.

Babin, Y., D'Amour, J., Pigeon, M., & Pēzolet, M. (1987) *Biochim. Biophys. Acta 903*, 78–88.

Boggs, J. M., & Rangaraj, G. (1983) *Biochemistry 22*, 5425–5435.

Borle, F., & Seelig, J. (1985) *Chem. Phys. Lipids 36*, 263–283.

Bush, S. F., Levin, H., & Levin, I. W. (1980) *Chem. Phys. Lipids 27*, 101–111.

Cameron, D. G., Casal, H. L., & Mantsch, H. H. (1980a) *Biochemistry 19*, 3665–3672.

Cameron, D. G., Casal, H. L., Gudgin, E. F., & Mantsch, H. H. (1980b) *Biochim. Biophys. Acta 596*, 463–467.

Cameron, D. G., Gudgin, E. F., & Mantsch, H. H. (1981) *Biochemistry 20*, 4496–4500.

Casal, H. L., & Mantsch, H. H. (1984) *Biochim. Biophys. Acta 779*, 381–401.

Casal, H. L., Mantsch, H. H., & Cameron, D. G. (1982) *J. Chem. Phys. 77*, 2825–2830.

Casal, H. L., Cameron, D. G., & Mantsch, H. H. (1983) *Can. J. Chem. 61*, 1736–1742.

Casal, H. L., Mantsch, H. H., & Hauser, H. (1987a) *Biochemistry 26*, 4408–4416.

Casal, H. L., Martin, A., Mantsch, H. H., Paltauf, F., & Hauser, H. (1987b) *Biochemistry 26*, 7395–7401.

Casal, H. L., Mantsch, H. H., Paltauf, F., & Hauser, H. (1987c) *Biochim. Biophys. Acta 919*, 275–286.

Cevc, G., Watts, A., & Marsh, D. (1980) *FEBS Lett. 120*, 267–270.

Chang, H., & Epand, R. M. (1983) *Biochim. Biophys. Acta 728*, 319–324.

Decius & Hexter (1977) *Molecular Vibrations in Crystals*, McGraw-Hill, New York.

Dluhy, R. A., Cameron, D. G., Mantsch, H. H., & Mendelsohn, R. (1983) *Biochemistry 22*, 6318–6325.

Eisenberg, M., Gresalfi, T., Riccio, T., & McLaughlin, S. (1979) *Biochemistry 18*, 5313–5323.

Eklund, K. K., & Kinnunen, P. K. J. (1986) *Chem. Phys. Lipids 39*, 109–117.

Eklund, K. K., Virtanen, J. A., Vuori, K., Patrikainen, J., & Kinnunen, P. K. J. (1987) *Biochemistry 26*, 7542–7545.

Farren, S. B., & Cullis, P. R. (1980) *Biochem. Biophys. Res. Commun. 97*, 182–191.

Fookson, J. E., & Wallach, D. F. H. (1978) *Arch. Biochem. Biophys. 189*, 195–204.

Hauser, H., & Shipley, G. G. (1981) *J. Biol. Chem. 256*, 11377–11380.

Hauser, H., & Shipley, G. G. (1983) *Biochemistry 22*, 2171–2178.

Hauser H., & Shipley, G. G. (1984) *Biochemistry 23*, 34–41.

Hauser, H., Paltauf, F., & Shipley, G. G. (1982) *Biochemistry 21*, 1061–1067.

Jähnig, F. (1976) *Biophys. Chem. 4*, 309–318.

Joutti, A., & Renkonen, O. (1976) *Chem. Phys. Lipids 17*, 264–266.

Kauppinen, J. K., Moffat, D. J., Mantsch, H. H., & Cameron, D. G. (1981) *Anal. Chem. 53*, 1454–1457.

Kinnunen, P. K. J., & Virtanen, J. A. (1986) in *Modern Bioelectrochemistry* (Gutmann, F., & Keyzer, H., Eds.) pp 457–479, Plenum, New York.

Koyama, Y., Yanagishita, M., Toda, S., & Matsuo, T. (1977) *J. Colloid Interface Sci. 61*, 438–445.

Laghdar-Ghazal, F., Tichadou, J.-L., & Tocanne, J. F. (1983) *Eur. J. Biochem. 134*, 531–537.

Levin, I. W. (1984) *Adv. Infrared Raman Spectrosc. 11*, 1–48.

Levin, I. W., Mushayakarara, E., & Bittman, R. (1982) *J. Raman Spectrosc. 13*, 231–234.

Lotta, T. I., Virtanen, J. A., & Kinnunen, P. K. J. (1988) *Chem. Phys. Lipids 46*, 13–23.

Mantsch, H. H., Hsi, S. C., Butler, K. W., & Cameron, D. G. (1983) *Biochim. Biophys. Acta 728*, 325–330.

Mushayakarara, E., & Levin, I. W. (1982) *J. Phys. Chem. 86*, 2324–2327.

Nielsen, J. R., & Hathaway, C. E. (1963) *J. Mol. Spectrosc. 10*, 366–377.

Pascher, I., Sundell, S., Harlos, K., & Eibl, H. (1987) *Biochim. Biophys. Acta 896*, 77–88.

Sacre, M. M., & Tocanne, J. F. (1977) *Chem. Phys. Lipids 18*, 334–354.

Seddon, J. M., Harlos, K., & Marsh, D. (1983) *J. Biol. Chem. 258*, 3850–3854.

Siminovitch, D. J., Wong, P. T. T., & Mantsch, H. H. (1987) *Biochim. Biophys. Acta 900*, 163–167.

Smirnova, E. Yu., Kozhomkulov, E. T., Vasserman, A. N., Vosnesensky, S. A., Shevchenko, E. V., Morozov, Yu. V., & Antonov, V. F. (1986) *Chem. Phys. Lipids 41*, 173–180.

Snyder, R. G. (1961) *J. Mol. Spectrosc. 7*, 116–144.

Snyder, R. G. (1967) *J. Chem. Phys. 47*, 1316–1360.

Snyder, R. G. (1979) *J. Chem. Phys. 71*, 3229–3235.

Snyder, R. G., & Schachtschneider, J. H. (1963) *Spectrochim. Acta 19*, 85–116.

Tasumi, M., & Shimanouchi, T. (1965) *J. Chem. Phys. 43*, 1245–1258.

Tocanne, J. F., Ververgaert, P. H. J. Th., Verkleij, A. J., & van Deenen, L. L. M. (1974) *Chem. Phys. Lipids 12*, 201–219.

Träuble, H. (1977) in *Structure of Biological Membranes* (Abrahamsson, S., & Pascher, I., Eds.) pp 509–550, Plenum, New York.

Träuble, H., Teubner, M., Wooley, P., & Eibl, H. (1976) *Biophys. Chem. 4*, 319–342.

Verkleij, A. J. (1984) *Biochim. Biophys. Acta 779*, 43–63.

Watts, A., Harlos, K., Maschke, W., & Marsh, D. (1978) *Biochim. Biophys. Acta 510*, 63–74.

Wilkinson, D. A., & Nagle, J. F. (1984) *Biochemistry 23*, 1538–1541.

Wilkinson, D. A., Tirrell, D. A., Turek, A. B., & McIntosh, T. J. (1987) *Biochim. Biophys. Acta 905*, 447–453.

Wohlgemüth, R., Waespe-Sarcevic, N., & Seelig, J. (1980) *Biochemistry 19*, 3315–3321.